

Time resolved spectroscopy of the variable brown dwarf Kelu-1[†]

F.J. Clarke^{1,2}, C.G. Tinney³ and S.T. Hodgkin²

¹European Southern Observatory, Alonso de Cordova 3107, Casilla 19001, Santiago 19, Chile

²Institute of Astronomy, Madingley Road, Cambridge CB3 0HA, UK

³Anglo-Australian Observatory, PO Box 296, Epping, NSW 2121, Australia

email: fclarke@eso.org, cgt@aoepp.aoa.gov.au, sth@ast.cam.ac.uk

26 November 2018

ABSTRACT

We report the results of observations designed to investigate the spectroscopic signatures of dust clouds on the L2 brown dwarf Kelu-1. Time resolved medium resolution spectra show no significant evidence of variability in the dust sensitive TiO, CrH and FeH bandheads on the timescale of 1–24 hours. We do however report periodic variability in the psuedo-equivalent width of H α consistent with the 1.8 hour rotation period previously reported for this object (Clarke, Tinney & Covey 2002). Near-contemporaneous *I*-band photometry shows evidence for non-periodic variability at the level of 2%.

Key words: techniques: spectroscopic, photometric — stars: low mass, brown dwarfs

1 INTRODUCTION

The brown dwarf Kelu-1 (Ruiz, Leggett & Allard 1997) is a L2 dwarf in the classification scheme of Kirkpatrick et al. (1999). With an effective temperature of \sim 1900K, refractory molecules such as TiO, CrH and FeH dominate the observed spectrum and play an important role in atmospheric physics. Clarke, Tinney & Covey (2002) (hereinafter CTC) have discovered periodic variability in photometric observations centred on the complex of molecular bandheads at \sim 8600Å. They provide several possible explanations for the variability, including: 1) dust cloud inhomogeneities modulating the surface brightness as Kelu-1 rotates (with an implied period of 1.8 hours), 2) A close substellar binary inducing ellipsoidal variability (implying an orbital period of 3.6 hours). In this paper, we report the results of a search for spectroscopic variability of Kelu-1 which answers this question.

Several spectroscopic searches have previously been made for variability in L and T dwarfs. Nakajima et al. (2000) found evidence for possible variability in the near IR water lines of the T dwarf SDSS1624+00, and Kirkpatrick et al. (2001) detected changes in the \sim 8700Å CrH feature of the L8 dwarf Gl 584C. With very similar aims to this study, Bailer-Jones (2002) has carried out near IR spectroscopic monitoring of the variable L1.5 brown dwarf 2MASSW J1145572+231730 (2M1145).

Photometric observations of 2M1145 show variability, but no evidence for periodicities, which Bailer-Jones & Mundt (2001a,b) claim as evidence for surface features evolving on the timescale of the rotation period. Spectroscopic observations spanning 54 hours do not show any evidence for variability. Bailer-Jones places an upper limit of 10–15% on the covering fraction of clear holes in a dusty photosphere (similar to our model 3 in §4.1).

In this paper we present the results of combined optical photometric and spectroscopic observations of Kelu-1 designed to test the causes of variability proposed by Clarke, Tinney & Covey (2002). Section 2 describes the data acquisition and reductions. Analysis of the resulting spectra and lightcurves are presented in section 3, and in section 4 we develop toy models to investigate our observations.

2 OBSERVATIONS AND DATA REDUCTION

2.1 Spectroscopy

Kelu-1 was observed on two consecutive nights (2002 February 13 and 14 UT) with the FORS2 instrument on VLT UT4 (Yepun). Both nights were photometric, with subarc-second seeing. A log of observations is given in table 1. The 300I grism and 1'' slit were used, providing a spectral resolution of \sim 13Å over the range 6300–11500Å. The OG570 order blocking filter was also used to remove second order light. The slit was aligned such that Kelu-1 and a brighter comparison star 25 arcsec to the south-west could be ob-

[†] Based on observations obtained at the European Southern Observatory, Paranal, Chile (ESO Programme 68.C-0381)

Date	UT time	Seeing	Sky conditions
2002 Feb 13	05:10–07:20	0.75–0.9"	Photometric
2002 Feb 14	05:22–07:15	0.75–1.0"	Photometric

Table 1. Log of FORS2 spectroscopic observations carried out on VLT UT4.

served simultaneously. Figure 1 shows the alignment of the slit, and identifies Kelu-1 and the comparison star. The two background stars seen near the slit in figure 1 are several arcseconds from the slit, and there is no detectable scattered light from them in our FORS2 spectra.

Each night's observations consisted of a two hour sequence of 480s integrations (for a total of 13 spectra per night). This gave us complete phase coverage of the 1.8 hour rotational period suggested by CTC, and provided enough signal to noise (~ 70 –80 per pixel; ~ 160 –180 per resolution element) to detect small changes between consecutive spectra. In addition to the science exposures, the ESO calibration plan provided lamp flats and observations of the spectrophotometric standard CD-32 9927 (Hamuy et al. 1994). Observations of the standard were taken about 1 hour after the science observations on night 2. HeAr arclamp exposures for wavelength calibration were also taken at the end of the 2nd night.

Observations were reduced with IRAF¹. After subtracting a bias frame, and correcting pixel-pixel variations and fringing with a normalized lamp flat, the spectra were extracted with APALL task using the optimal extraction method of Horne (1986). The spectra were wavelength calibrated via the HeAr arc spectra. To keep the spectra as “raw” as possible, we did not interpolate them onto a linear scale. The night sky lines show that the wavelength solution is stable during each night, but changes by $\sim 4\text{\AA}$ between the nights. The spectrophotometric standard was then used to correct the illumination function of the instrument. Figure 2 shows the averaged spectrum of Kelu-1 from the 1st night.

2.2 Photometry

I-band photometry of Kelu-1 was obtained in service mode with the EMMI instrument at the NTT on the nights of 2002 February 17 and 19 UT. ESO filter #610 was used, which is slightly redder than the standard Cousins *I*_c filter. For the rest of this paper, we have used the ESO #610 filter profile when discussing the “*I*” filter. The CCD chip was windowed to give a $3.2' \times 3.2'$ field of view. To further reduce readout overheads we employed 2×2 pixel binning, giving a pixel scale of $0.54''/\text{pixel}$. The observations consisted of consecutive 120 second exposures over two hours, with around forty frames obtained each night.

Data were reduced in the standard fashion with IRAF, subtracting a bias frame and dividing by a normalized dome flat. Aperture photometry was then performed on the target and a selection of comparison stars with the APPHOT package within IRAF. Differential lightcurves

¹ The Image Reduction and Analysis Facility (IRAF) is distributed by NOAO, which is operated by AURA, Inc., under contract to the NSF.

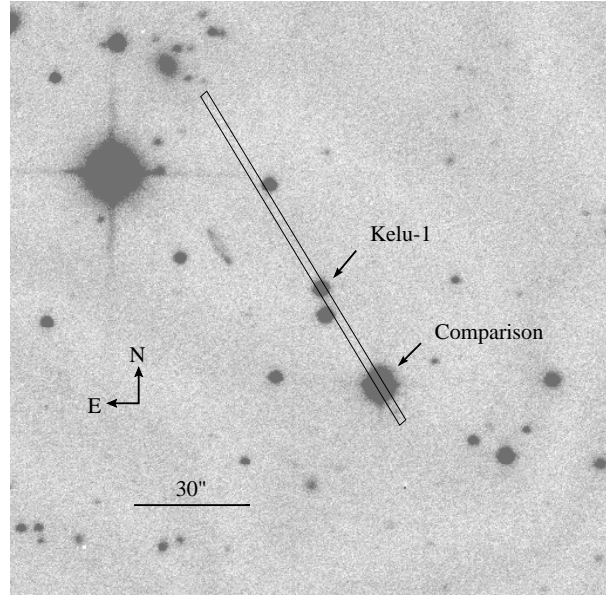


Figure 1. Slit position on the sky of the FORS observations showing the position of Kelu-1 and the comparison star.

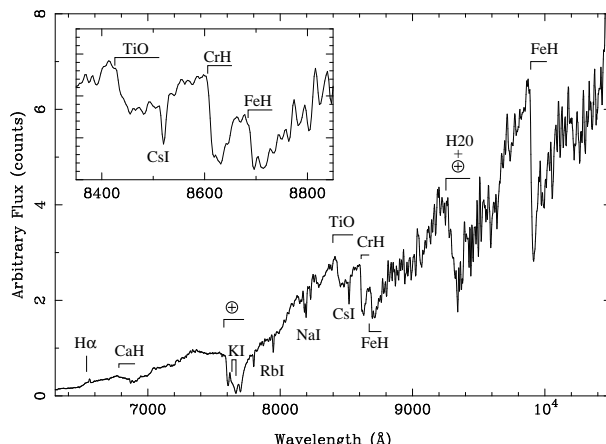


Figure 2. Spectrum of Kelu-1 with important atmospheric features denoted. The insert panel shows a close up of the molecular complex at $\sim 8600\text{\AA}$

(target–comparison) were then constructed in the manner described by Clarke, Oppenheimer & Tinney (2002). Briefly, we produce a mean comparison star from an ensemble of non-variable stars in the field, and it is this “mean” that we refer to as the comparison star in §3.1.

3 RESULTS

3.1 *I*-band photometry

Figure 3 shows the differential *I*-band lightcurve of Kelu-1 minus comparison star (upper panel) and comparison minus check star (lower panel). Table 2 gives the statistics of the lightcurves. The rise of 0.02 mag in the Kelu-1 lightcurve from 4.34 to 4.36 (~ 30 minutes) is significant at the 4-sigma level. The comparison minus check lightcurve remains con-

Lightcurve	Mean		Standard Dev		Average Dev	
	night 1	night 2	night 1	night 2	night 1	night 2
Kelu-1 – Comp	-0.0082	0.0117	0.0069	0.0054	0.0049	0.0042
Check – Comp	-0.0013	0.0012	0.0078	0.0065	0.0057	0.0045

Table 2. Statistics for Kelu-1 NTT differential photometry. The mean for each night is mean magnitude of that night's data relative to the mean magnitude of the whole dataset. Standard deviation is defined as $\sqrt{\frac{1}{N-1} \sum (x_i - \bar{x})^2}$ and the average deviation is defined as $\frac{1}{N} \sum |x_i - \bar{x}|$.

stant to 0.002 mag during this time. This rise represents a dimming of Kelu-1.

Periodogram analysis of the data does not show evidence for any significant periods, but the analysis is heavily compromised by the window function of the data. They are however, inconsistent with the 1.8 hour (and 3.6 hour) period found in the 2000 photometry. As discussed later (§3.3), there is evidence from the spectroscopy to support the interpretation of the 1.8 hour period as the rotation period. The *I*-band and R6 filter used by CTC ($\lambda_{cen} = 8580\text{\AA}$, $\Delta\lambda = 410\text{\AA}$) should react similarly to inhomogeneities in the atmosphere (see Figure 11 and §4.1), so we must assume that the atmosphere of Kelu-1 has evolved significantly between March 2000 and February 2002. It may be that in March 2000, Kelu-1 had a significant long lived (>25 rotations) surface feature, which has since dissipated. In February 2002, if stable features were present, they were smaller and affected the lightcurve at less than the 0.5% level. The 0.02 mag dimming may be due to more rapid evolution of a surface feature, as has been claimed for other brown dwarfs (Bailer-Jones & Mundt 2001a; Bailer-Jones & Mundt 2001b).

3.2 Dust sensitive spectroscopic features

At the temperature of Kelu-1's photosphere ($T_{eff} \simeq 1900\text{K}$) gas phase molecules begin to condense into solids (i.e. dust). The removal of species like Ti, V, Fe and Cr from the gas phase into solids results in the weakening of TiO, VO, FeH and CrH bands. If Kelu-1's photosphere has significant spatial dust inhomogeneities, we may expect to see the signature in these lines (see §4.1). The complex of lines around 8700\AA (TiO, CrH and FeH) is particularly interesting, as these lines dominate the photometric band in which CTC detected variability.

Figure 4 shows the time series spectra of the $8200\text{--}8900\text{\AA}$ region, and does not show any obvious evidence for variability. To make any small differences more apparent to the eye, we have plotted the difference spectra of this region in figure 5. An average spectrum has been constructed for each night, and this has been subtracted from each individual spectrum. In both plots, each spectrum has been offset for clarity, with time increasing from the top of the diagram. The offsets between consecutive spectra are constant however, and do not represent the actual time between observations. There does not appear to be any evidence for variability of the molecular bands either between or during each night.

To test for subtle changes in the absorption depth, we have measured the flux ratio between narrow bands straddling the molecular bandheads. These bands are shown in right-

Band	λ_{cen}	$\Delta\lambda$
TiO1	8395	50
TiO2	8485	50
CrH1	8580	40
CrH2	8628	16
FeH1	8670	20
FeH2	8710	20

Table 3. Bands used to measure the depth of molecular absorption features.

hand panel of figure 4 and described in table 3. The flux through each band was summed, and the molecular band index is defined as the ratio of the fluxes, i.e. TiO index = TiO1/TiO2. To check for instrumental or atmospheric effects, we also measured band indices for the comparison star, although no molecular absorption is seen in this object. Figure 6 shows the TiO, CrH and FeH indices during the observations for Kelu-1 (upper panels) and the comparison star (lower panels). Errors are carried through from the error estimates produced by APALL. The band indices for all these molecules are constant to within $\pm 2\%$. The most significant indication of variability is in CrH between the nights. This is significant at the 3σ level, but the fact that similar effects are seen in the comparison star leads us to believe we are not observing effects intrinsic to Kelu-1. The 1σ upper limits on variability (peak-to-peak) of the molecular band indices are; TiO $< 1.4\%$, CrH $< 4\%$, FeH $< 2.2\%$.

3.3 $\text{H}\alpha$ Variability

The $\text{H}\alpha$ data show evidence for significant variability on even a cursory examination. Figure 7 shows a close up the $\text{H}\alpha$ line from all the spectra. Each spectrum has been offset for clarity, in the same fashion as figure 4.

We have measured the pseudo equivalent width (PEW) of the $\text{H}\alpha$ line in all the spectra with the splot task in IRAF. The results are plotted in figure 8 as PEW($\text{H}\alpha$) as a function of time. It is clear from this plot that the PEW($\text{H}\alpha$) changes with time. Periodogram analysis reveals a period in the range 1.5–2.5 hours – consistent with the 1.8 hour photometric period reported by CTC. The broad peak in the periodogram is due to the limited time coverage on each night. Figure 9 shows the PEW($\text{H}\alpha$) folded on a period of 1.8 hours. The central wavelength of the $\text{H}\alpha$ line does not change significantly throughout the observations.

The mean level of PEW($\text{H}\alpha$) is $\sim 3.0\text{\AA}$ (in emission), which is slightly larger than, although comparable to previously measured values (e.g. $1.5\text{--}2.0\text{\AA}$;

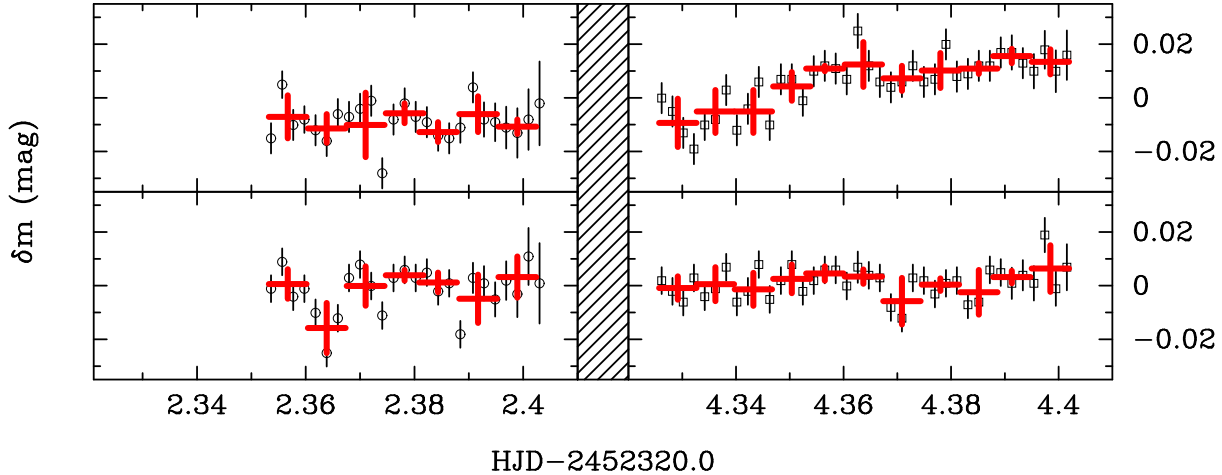


Figure 3. *I*-band lightcurve of Kelu-1 on 2002 February 17 and 19 UT. The upper panel shows Kelu-1 minus comparison star, and the lower panel shows comparison minus check star. Each lightcurve has been mean subtracted (using data from both nights). The thick bars show the photometry averaged into 10 minute bins.

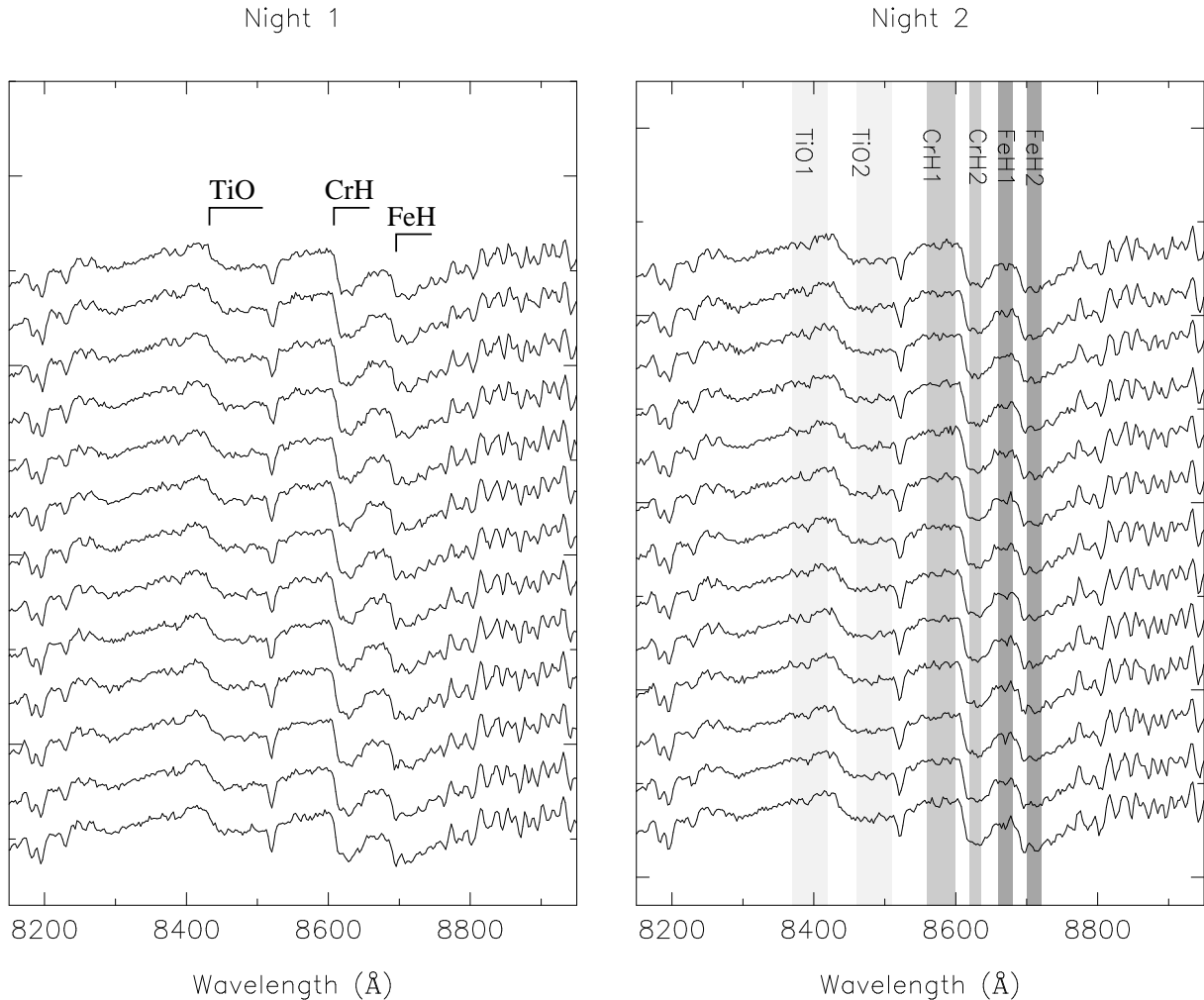


Figure 4. Time series spectra of the molecular lines of TiO, CrH and FeH at 8400–8800Å. Time increases downwards, but the plotted gap does not represent the actual time between observations. In the right panel (night 2), we have marked the bands used to measure the strength of the absorption features (Table 3)

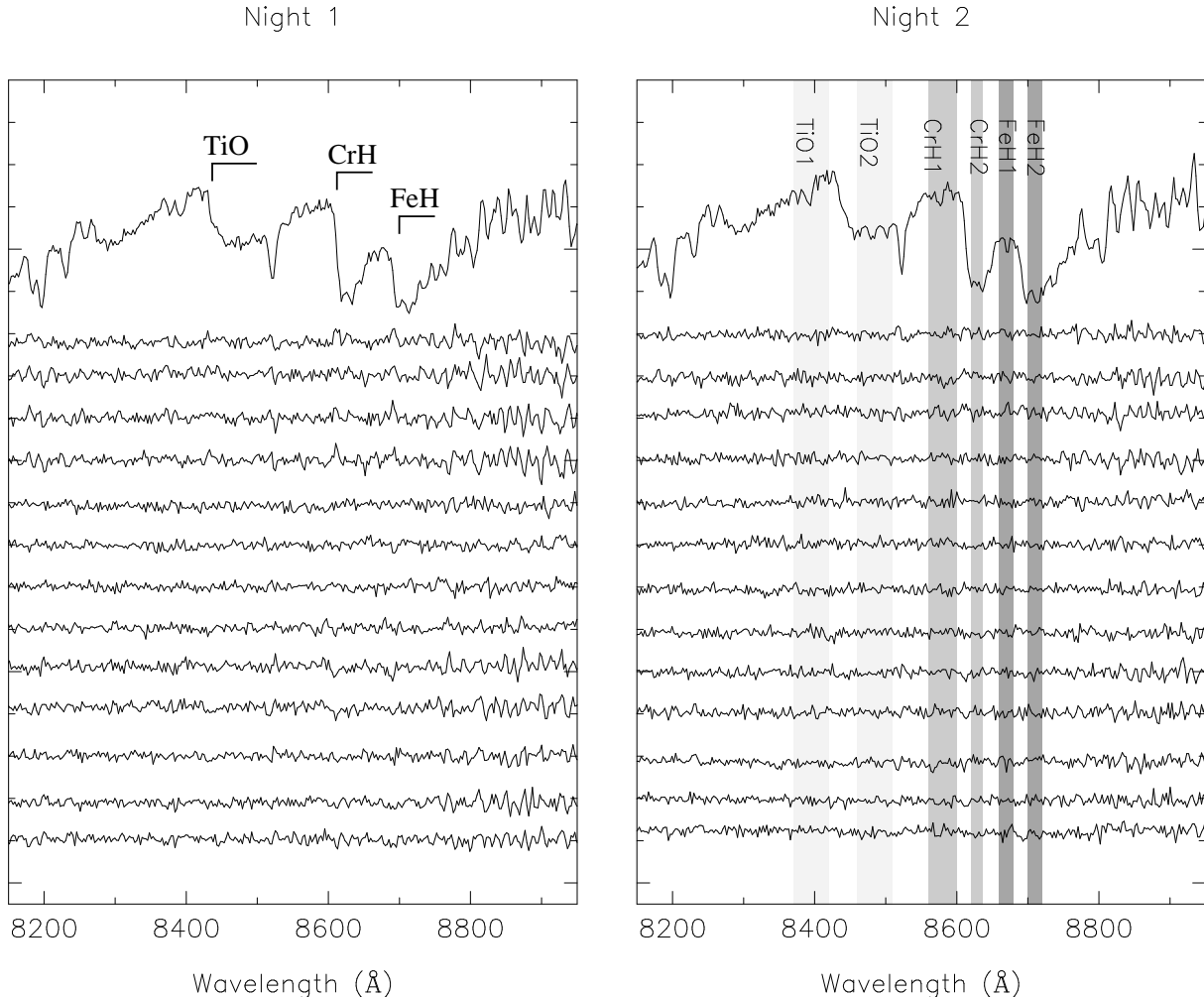


Figure 5. Difference spectra of the molecular lines of TiO, CrH and FeH at 8400–8800Å. Each spectrum has had the average of all the night’s spectra (upper most spectrum) subtracted. The increased noise redward of 8800Å is due to a combination of telluric variability and lower S:N in this region ($\sim 75\%$ of the SN at 8600Å).

Basri 2001, Kirkpatrick et al. 1999). We have also measured the flux in the H α line with SPLOT. The mean H α line flux during our observations was $0.8 \pm 0.4 \times 10^{-16}$ erg/s/cm 2 , comparable with the value reported by Ruiz, Leggett & Allard (1997). To check the flux calibration of our spectroscopy, we have calculated the flux through the *I* bandpass. This is $\sim 75\%$ higher than expected (given Kelu-1’s *I* band magnitude of 16.8, Ruiz, Leggett & Allard 1997), but the discrepancy is probably due to overestimate of flux towards the red end of the spectrum, where the standard star is very faint. We therefore assume a conservative error of 50% in our line flux (included above).

3.4 Radial velocity changes

To look for changes in Kelu-1’s radial velocity, we have measured the wavelength of the strong neutral atomic lines of RbI (7800, 7948Å) and CsI (8521Å). These lines lie in relatively “clean” areas of the spectrum and, unlike the close doublets of KI and NaI, allow simple single profile fitting. We used the splot task in IRAF to do this. To check for instrumental drifts, we measured the central wavelength of

several lines in the comparison star. For each line, we convert the measured wavelength to a velocity relative to the mean wavelength of the line in all spectra. All the lines are then averaged to give a radial velocity for each spectrum. Figure 10 shows the radial velocity curves for Kelu-1 (upper panel) and the comparison star (lower panel). The same trend is seen in both stars, indicating the observed velocity changes are instrumental effects. This is most likely caused by drifts in the centering of the stars on the slit, which was typically wider than the FWHM. The scatter on the velocity measurements of Kelu-1 is ± 10 kms $^{-1}$. This provides an upper limit on radial velocity variations, and rules out a close companion with $M \sin i > 10 M_{\text{jup}}^2$ ². We can therefore reject the binary hypothesis for Kelu-1’s variability proposed by CTC. Note also that the lack of a 1.8 hour period in the *I*-band photometry also rules out a companion as the source of variability, as a companion would produce consistent and repeatable variability.

² Assuming a mass of $0.065 M_{\odot}$ for Kelu-1

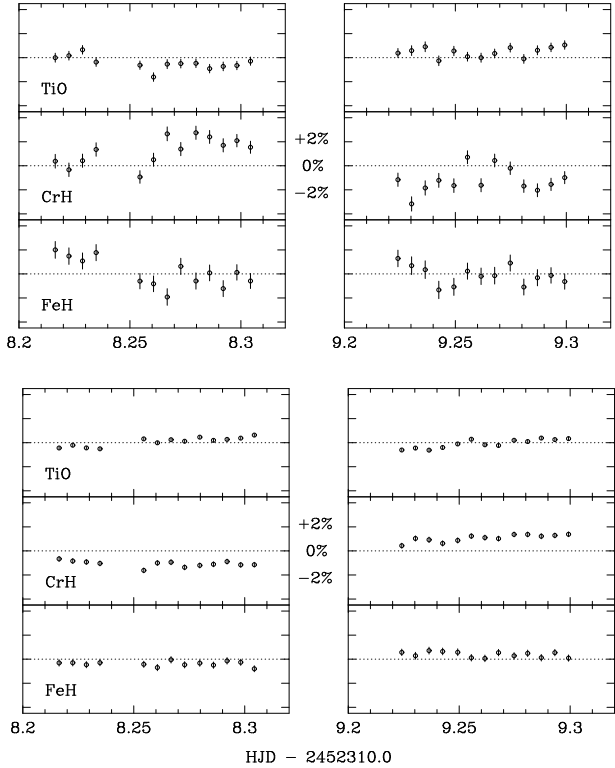


Figure 6. Changes in the molecular band strengths during the observations for Kelu-1 (upper panels) and the comparison star (lower panels). The definition of band strength of given in the text.

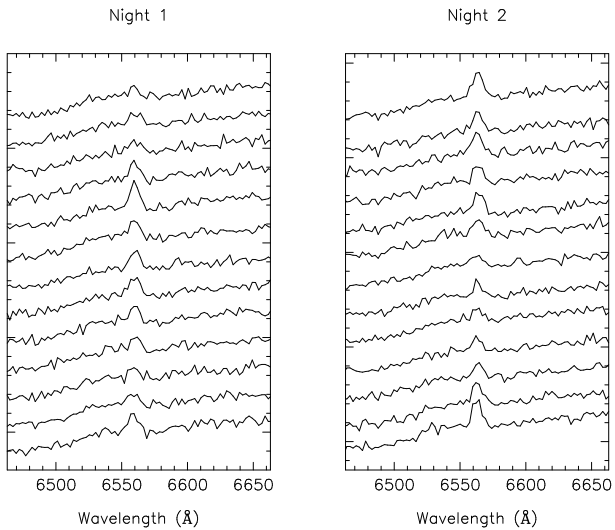


Figure 7. Close ups of the H α line. The first night is shown on the left, and the second night on the right. The spectra have been offset for clarity, with the earliest spectra in each night top of each panel.

4 DISCUSSION

4.1 Limits on the inhomogeneity of Kelu-1's atmosphere

Allard et al. (2001) provide theoretical spectra for models relating to the two limiting cases of dust formation. The

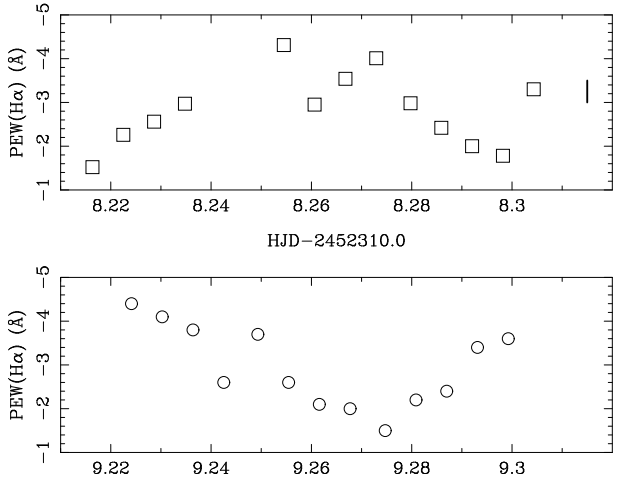


Figure 8. PEW(H α) during the FORS observations. The upper panel shows night 1, and the lower panel night 2. Typical errors on the PEW(H α) are 0.5Å, as shown by the vertical line in upper panel.

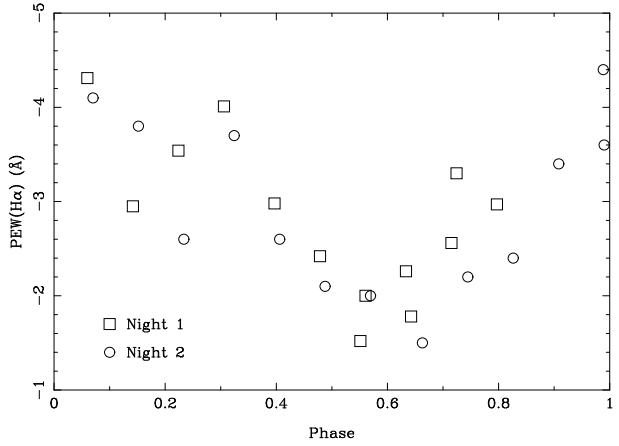


Figure 9. PEW(H α) folded on the period of 1.8 hours reported by CTC. This period is consistent with a periodogram analysis of the PEW(H α) data itself.

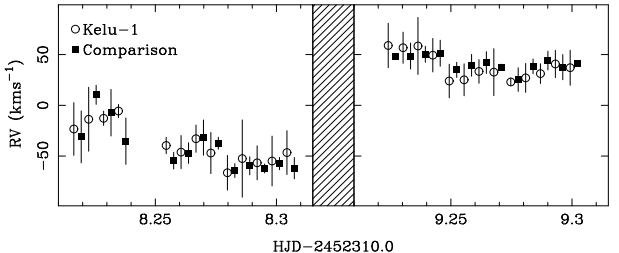


Figure 10. Radial velocity measurements of Kelu-1 (empty circles) and the comparison star (filled squares). The times of the comparison star points have been slightly offset for clarity. Each measurement is the average of several lines, and the error bars are given by the standard deviation.

DUSTY model assumes that dust forms and remains suspended evenly throughout the photosphere, analogous to small grains supported in thermal updrafts. Alternatively, in the COND model, dust particles form but immediately settle below the photosphere - a good model for grains which are too large to be supported by convective updrafts. In reality, the detailed physics of dust formation in substellar atmospheres is much more complex, being a coupled system involving chemistry, atmospheric dynamics, radiative transfer and cloud formation. In particular, gravitational settling of dust grains and thermal structure in the atmosphere will lead to a vertically stratified distribution of dust. Several groups (Ackerman & Marley 2001, Cooper et al. 2002, Tsuji 2002, Marley et al. 2002) have made more detailed attempts to model dust formation in substellar atmospheres. All models to date, however, are static, and do not treat any horizontal inhomogeneities in atmospheric structure.

To make a crude estimate of the effects a “patchy” photosphere would have on the emergent spectrum, we can combine the DUSTY and COND models. The overall spectrum of Kelu-1 is best fit by a DUSTY model at 1900K (Baraffe et al. 1998), so we assume that inhomogeneities are best modeled by COND “holes” in an otherwise DUSTY photosphere. By definition, holes will allow us to see into deeper, hotter regions of the photosphere. With this in mind, we have constructed several models;

Model-1 2100K COND holes representing patches of efficient dust settling which allow us to see deeper into the atmosphere.

Model-2 2100K DUSTY holes representing patches which allow us to see a deeper level of the atmosphere, but where dust is still significant.

Model-3 1900K COND holes representing patches of efficient dust settling at the same temperature as the rest of the photosphere.

In all cases, the 1900K DUSTY spectrum represents the majority of the photosphere. To model the effects of inhomogeneities in the atmosphere, we construct a linear combination of the two spectra as;

$$f(\lambda)_{\text{mix}} = (1.0 - F)f(\lambda)_{\text{phot}} + Ff(\lambda)_{\text{hole}} \quad (1)$$

where $f(\lambda)_{\text{phot}}$ and $f(\lambda)_{\text{hole}}$ are the model spectra representing the normal and “hole” regions of the atmosphere, and F is the covering fraction of holes. We therefore generate a “mixed” spectrum, for which we can measure molecular band indices in exactly the same way as for the real data (§3.2). We also measure the photometric bands I (ESO #610) and $R6$ (as used by CTC; $\lambda_{\text{cen}} = 8580\text{\AA}$, $\Delta\lambda = 410\text{\AA}$).

Figure 11 shows the effects of changing the “hole” covering fraction for all three models. The band indices are normalised to the purely dusty case (no holes, $F = 0$), so the points give the change in band indices we would observe if the photosphere changed from having no holes, to having a given covering fraction. The effect of small changes in F is roughly linear, so the plots are also valid for a changes between two non-zero covering fractions.

The horizontal shaded area shows the $R6$ photometric amplitude reported by CTC ($1.2 \pm 0.1\%$). The most striking feature of these plots is the incredibly small changes in cov-

ering fraction (vertical shaded area) required to reproduce the observed photometric variability; less than 2% “holes” in all three models. Comparing with the molecular band indices, our upper limits on variability ($\text{TiO} < 1.4\%$; $\text{CrH} < 4\%$; $\text{FeH} < 2.2\%$) are entirely consistent with these covering fractions for all models. It should be noted however, that these limits represent the *difference* in covering fraction between one side of the brown dwarf and the other, the atmosphere may be far more inhomogeneous on small scales.

Comparing the models reveals interesting differences between them. The CrH index appears to be much more sensitive to dust properties (models 1 & 3) rather than temperature (model 2). The TiO index offers a potential discriminant between models 1 & 3, becoming stronger with covering fraction in model 1, and weaker in model 3. None of the molecular bands are strongly effected in model 2, which depends purely on temperature. The fact that the scatter in our measurement of CrH is larger than TiO and FeH is more in line with models 1 and 3 than model 2. However, the most probable explanation of differences between the models is that our toy models are too primitive to throw any light onto these subtle effects. It is likely a full 3-dimensional model of a brown dwarfs atmosphere will be required to interpret the results of future spectroscopic studies.

4.2 The chromosphere of Kelu-1

The $\text{H}\alpha$ emission we see is probably caused by ionised hydrogen gas in Kelu-1’s chromosphere, analogous to other low mass stars (e.g. Gizis et al. 2000). The energy required to heat the gas may come from magnetic heating (Mohanty et al. 2002), or wave heating (Yelle 2000), although calculations of the energy released from both are problematic. Combined with magnetic fields above the surface of Kelu-1, this could lead to inhomogeneous patches of hot gas above Kelu-1 and produce the variable $\text{H}\alpha$ emission we observe. Similar periodic $\text{H}\alpha$ variability has been observed from other stars. Fernández & Miranda (1998) show the variable $\text{H}\alpha$ emission from several weaklined T-Tauri stars is correlated with photometric variability, which they interpret as chromospheric magnetic loops corotating above cool magnetic spots in the photosphere. Similar anchored magnetic loops could exist above Kelu-1, leading to $\text{H}\alpha$ variability with the same (rotation) period as photospheric variability.

The presence of magnetic fields and a chromosphere do not necessarily contradict previous arguments against magnetic spots in the photospheres of ultra cool dwarfs (Bailer-Jones & Mundt 2001a; Gelino et al. 2002; Mohanty et al. 2002; Bailer-Jones 2002). Densities in the region of the photosphere are much higher, and the atmosphere there is much more neutral. This corresponds to very low magnetic Reynolds numbers (Gelino et al. 2002), or high electrical resistivities (Mohanty et al. 2002). In the region of the photosphere, the magnetic field is decoupled from the atmospheric fluid. A magnetic field may be generated deeper in the atmosphere, where the temperature and ionisation fraction rise, and the magnetic field is well coupled to the matter.

The $\text{H}\alpha$ line flux we measured in §3.3 corresponds to an $\text{H}\alpha$ luminosity of $3.7 \pm 1.8 \times 10^{24} \text{ erg/s/cm}^2$ at Kelu-1’s distance of 19.6 pc (Dahn et al. 2002). In the standard mea-

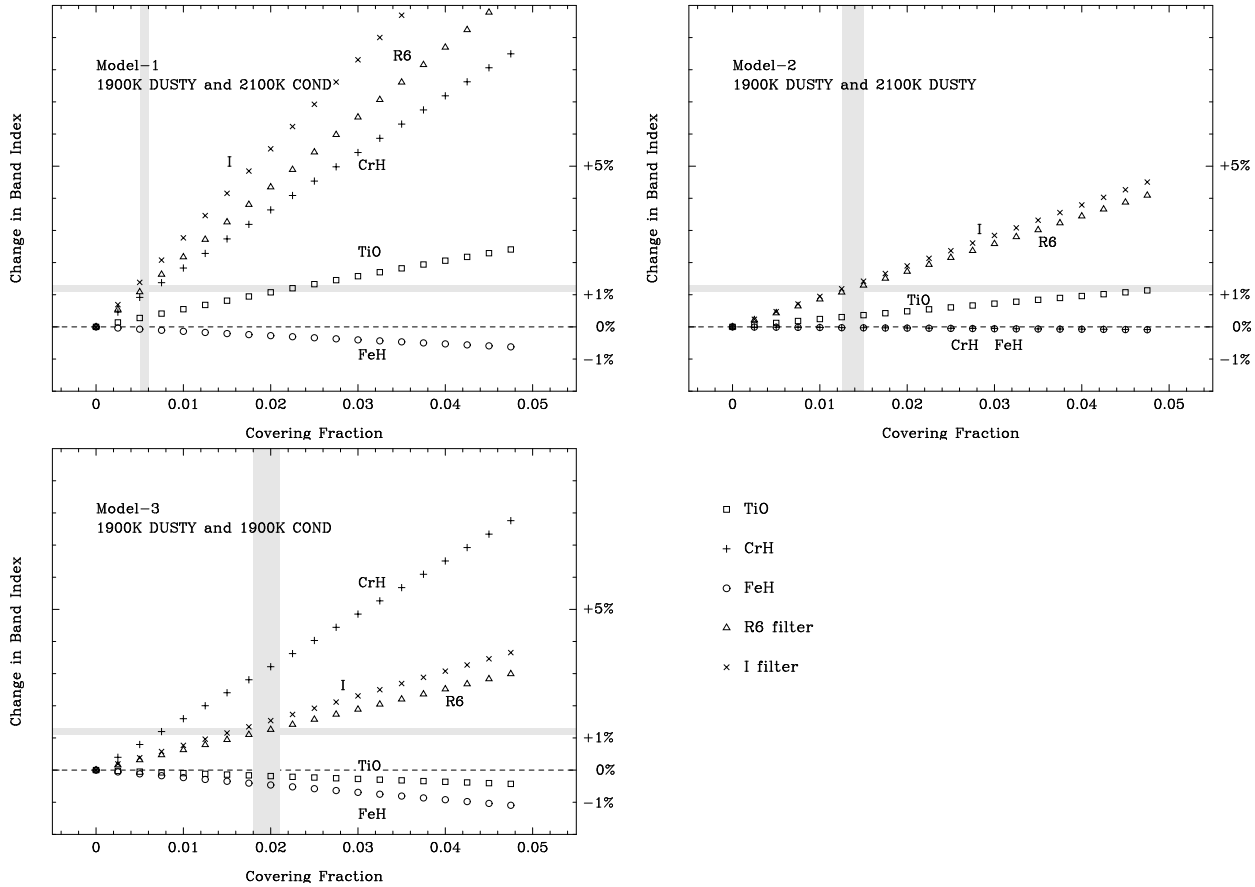


Figure 11. Changes in band strength with covering fraction for all three models. Model-1 upper left, Model-2 upper right and Model-3 lower left. The shaded areas in each plot represent the amplitude of the R6 variability discovered by CTC ($1.2 \pm 0.1\%$), and the corresponding surface covering fraction. A covering fraction of 0 represents a photosphere with no “holes”.

sure of chromospheric activity, Kelu-1 has $\log(L(H\alpha)/L_{\text{bol}})$ of -5.35 ± 0.5 , where our error estimates are quite conservative (§3.3). This value is in line with what we would expect for a L2 dwarf from the work of Gizis et al. (2000) and Mohanty et al. (2002).

5 CONCLUSIONS

We have presented here the first high signal-to-noise phase resolved optical spectroscopy of a brown dwarf with a known rotation period. We have detected a rotational modulation of the $H\alpha$ line, consistent with the 1.8 hour rotation period reported by Clarke, Tinney & Covey (2002). Radial velocity measurements reject the possibility that photometric variability is caused by a close companion to Kelu-1. Photometry shows that the atmosphere of Kelu-1 has significantly evolved between March 2000 and February 2002, when no periodic signal can be detected at the level of 0.5%. Kelu-1 does however show evidence for a 2% dimming over ~ 30 minutes. We have also placed upper limits on the scale of possible surface features inducing inhomogenous dust formation across the surface, and made a primitive attempt to investigate the effects of different atmosphere models. On the balance of observations, it seems that Kelu-1 is a single brown dwarf, with a typical level of chromospheric activ-

ity, and a relatively homogenous, although evolving, atmosphere.

6 ACKNOWLEDGEMENTS

We would like to thank the staff of the VLT and NTT for their help in making these observations, especially for rearranging at short notice the NTT queue to allow quasi-simultaneous observations. We also thank the referee, Coryn Bailer-Jones, for his timely response and useful comments. FJC acknowledges the support of a PPARC studentship award during the course of this research.

REFERENCES

- Ackerman A. S., Marley M. S., 2001, ApJ, 556, 872
- Allard F., Hauschildt P. H., Alexander D. R., Tamanai A., Schweitzer A., 2001, ApJ, 556, 357
- Bailer-Jones C. A. L., Mundt R., 2001, A&A, 367, 218
- Bailer-Jones C. A. L., Mundt R., 2001, A&A, 374, 1071
- Bailer-Jones C. A. L., 2002, A&A, 389, 963
- Baraffe I., Chabrier G., Allard F., Hauschildt P. H., 1998, A&A, 337, 403
- Basri G., 2001, in ASP Conf. Ser. 223: 11th Cambridge Workshop on Cool Stars, Stellar Systems and the Sun. p. 261

Clarke F. J., Oppenheimer B. R., Tinney C. G., 2002, MNRAS, 335, 1158

Clarke F. J., Tinney C. G., Covey K. R., 2002, MNRAS, 332, 361

Cooper C. S., Sudarsky D., Milsom J. A., Lunine J. I., Burrows A., 2002, astro-ph/0205192

Dahn C. C. et al., 2002, AJ, 124, 1170

Fernández M., Miranda L. F., 1998, AA, 332, 629

Gelino C. R., Marley M. S., Holtzman J. A., Ackerman A. S., Lodders K., 2002, ApJ, 577, 433

Gizis J. E., Monet D. G., Reid I. N., Kirkpatrick J. D., Liebert J., Williams R. J., 2000, AJ, 120, 1085

Hamuy M., Suntzeff N. B., Heathcote S. R., Walker A. R., Gigoux P., Phillips M. M., 1994, PASP, 106, 566

Horne K. D., 1986, PASP, 98, 609

Kirkpatrick J. D. et al., 1999, ApJ, 519, 802

Kirkpatrick J. D., Dahn C. C., Monet D. G., Reid I. N., Gizis J. E., Liebert J., Burgasser A. J., 2001, AJ, 121, 3235

Marley M. S., Seager S., Saumon D., Lodders K., Ackerman A. S., Freedman R. S., Fan X., 2002, ApJ, 568, 335

Mohanty S., Basri G., Shu F., Allard F., Chabrier G., 2002, ApJ, 571, 469

Nakajima T. et al., 2000, PASJ, 52, 87

Ruiz M. T., Leggett S., Allard F., 1997, ApJL, 491, L107

Tsuji T., 2002, ApJ, 575, 264

Yelle R., 2000, in ASP Conf. Ser. 212: From Giant Planets to Cool Stars. p. 267